Mixing and Intrusions in a Rotating Cold-Core Feature off Cape Blanco, Oregon

JAMES N. MOUM AND DOUGLAS R. CALDWELL

College of Oceanography, Oregon State University, Corvallis, Oregon

PHYLLIS J. STABENO

Pacific Marine Environmental Laboratory, Seattle, Washington

(Manuscript received 26 May 1987, in final form 3 December 1987)

ABSTRACT

During August 1986, a large cold anomaly was observed in satellite and in situ measurements near Cape Blanco at 42°N, 126°30′W off the Pacific Coast. Detailed vertical profiles of temperature, conductivity, turbulent dissipation, and horizontal currents showed 1) surface water temperature changes as large as 2 degrees in 1 kilometer (but smaller gradients at depth); 2) a structure in the mean currents resembling that of either a cyclonic eddy or a current meander; 3) a current field in geostrophic balance on scales of 10 km and greater; 4) a region of intrusions on the northern side of the eddy; 5) a concentration of turbulence (as indicated by the kinetic-energy dissipation rate) on the edges of the eddy and in the region of intrusions, the core of the eddy being turbulence-free; and 6) a substantial change in the surface structure in 24 hours.

1. Introduction

Off the West Coast of the United States during the upwelling season (spring and early summer), anomalously cool (1–4°C) features extending 100 to 300 km offshore are often seen in infrared images of the ocean surface derived from satellite measurements (Bernstein et al. 1977; Mooers and Robinson 1984; Ikeda and Emery 1984, for example). Some of these observations have been confirmed by on-site shipboard measurements of hydrography and currents (Mooers and Robinson 1983; Reinecker et al. 1985; Flament et al. 1985; Kosro and Huyer 1986). All the on-site measurements have been made off Point Arena and the authors have presented conceptual models of jetlike cold features moving offshore.

While conducting engineering tests of improvements to our underway microstructure instrument the Rapid Sampling Vertical Profiler (RSVP) off Cape Blanco on the coast of Oregon in August 1986, we encountered a cold, *rotational* feature marked by sharp sea-surface temperature boundaries. It was a density anomaly whose density differential was enhanced by salinity as well as its temperature. We crossed it once while making closely spaced microstructure and horizontal current profiles. A second, faster transect, with current and SST measurements only, was made to determine its short-term evolution.

Corresponding author address: Dr. James N. Moum, College of Oceanography, Oregon State University, Corvallis, OR 97331.

The Cape Blanco feature shares the characteristic of a cold core with the Point Arena features, and has comparable scales (100 km horizontal, 300 m vertical). It is asymmetric, with its sharp side to the north, which was a site for strong offshore flow, but it differs in other characteristics. Notably, the salinity anomaly reinforces the density contrast to make its total density contrast twice that of the largest density contrast in the Point Arena features. More importantly, it appears to be highly rotational.

One interesting aspect of the microstructure measurements is that regions of large kinetic-energy dissipation rate occurred near the surface, at the edges of the strongest velocity jets within the feature and at the boundaries of the feature associated with thermohaline intrusions. In a large region ($\approx$50 km) at the core, vertical mixing was weak; turbulent dissipation rates there were at or below the noise level of our instrumentation (10^{-9} m^2 s^{-3}).

The cold region had the odor of fish, indicating that biological productivity was stronger there. The northern frontal boundary was a site for elongated (in the along-front direction) slicks through which a large school of porpoises were hunting. The across-front width of the hunting region was only a kilometer or so, situated on the frontal boundary.

In the following pages we briefly describe the instrumentation, discuss the large-scale structure and then the smaller-scale structure, focusing first on one of the frontal boundaries and then on a large thermohaline intrusion. A rapid evolution of the near-surface waters is documented from the data of the second transect.

2. Instrumentation and data processing

Continuous records of wind, sea surface temperature (SST), and electrical conductivity (temperature and conductivity from the sea chest) were obtained using the sensors resident aboard the R/V *Thomas G. Thompson*. (The sea-chest temperatures were almost 0.5°C higher than the profiler temperatures. The latter are regarded as correct because of careful calibration and favorable comparison with CTD profiles. No correction was made for this constant offset.)

a. Rapid Sampling Vertical Profiler (RSVP)

The Rapid Sampling Vertical Profiler (RSVP; Caldwell et al. 1985) was designed for fast, intensive surveys of hydrographic structure and microstructure parameters in the upper ocean. Sensors mounted on the nose of the freely-falling vehicle determine temperature, conductivity, and velocity microstructure from which we estimate the rate of dissipation of turbulent kinetic energy (Osborn and Crawford 1980). A total of 117 vertical profiles were made during the first southward transect of the cool anomaly off Cape Blanco on 23 and 24 August, at a mean spacing of approximately 2 km.

b. Acoustic Doppler current profiler (ADCP)

The hull-mounted RD 150 kHz acoustic Doppler current profiler (ADCP) was tuned (using software and firmware developed by RD Instruments) to transmit 4 m pulses and gate 4 m return bins. The 80-bin limit on the RD software covers only the upper 329 m. Due to acoustic noise near the source, the first two bins were not analyzed and the first useful bin was centered at 17 m. The relative velocity profiles were time-averaged over 5 minutes before further processing.

To obtain absolute velocities from the ADCP relative velocity estimates, ship motion was removed using Loran-C navigation. Loran-C coordinates (at 5-minute intervals) were differenced and smoothed (using a ½-hour filter) to obtain ship velocities. The ADCP velocities were smoothed with a matching filter and the two velocity series were added to derive absolute velocities. A second 1-hour filter was then applied. We judge the errors in the final velocity estimates to be less than 5 cm s^{-1}. We have no independent velocity measurements to compare with these estimates, but successive transects in opposite directions and at different ship speeds compare within that error.

3. Large-scale structure

At 1600 UTC 23 August 1986, we steamed from 43°20′N due south at 4.5 knots along 126°30′W (Fig. 1), with the ADCP operating and RSVP casts extending to depths of 150 to 200 m. We continued for 28 hours, reaching 41°15′N. The sea surface temperature (Fig. 2) and ADCP currents (Fig. 4) indicated that we were passing through a large (100 km), cold core feature (3° to 4°C temperature difference) distinguished by rapidly moving surface frontal boundaries. We will refer to the cold core feature found on this transect as the CCF.

Attempts to identify this feature in satellite infrared imagery were hampered by cloud cover. The clear image closest in time was made on 20 August, 3.5 days before the transect (Fig. 1). The horizontal scale and the temperature difference across the feature centered just south of Cape Blanco (Fig. 1) match those found during the shipboard transect (Fig. 2), and the location of the cold feature in the satellite image matches approximately. It is likely that these are signatures of the same feature in different stages of evolution. A number of other features appear in Fig. 1. Along the edge of the cloud band and north of 43°N, numerous smaller features (horizontal scales $\approx$ 10 km) lie along the sharp warm/cool water boundary. A long, cool tendril north of the feature off Cape Blanco apparently ends in an isolated pool O(10 km) of cool water at 43°N, 127°30′W. Just to the north of Cape Mendocino at 41°N, a large body of cool surface water is marked by highly irregular frontal boundaries and a much more diffuse southern boundary (compared to its northern boundary). In contrast to the other features, the cold anomaly off Cape Blanco is distinguished by its very regular structure and frontal boundaries.

The most immediate manifestation of the cold core feature (CCF) was the strong SST signature (Fig. 2). It was initially recognized by the sharp (2.5°C in 1500 m) northern front between the 16.5° to 17.5°C water to the north and the internal 13° to 14.5°C water. The southern front was considerably more diffuse. Our knowledge of the two-dimensional horizontal structure of the feature is limited to the satellite image obtained 3.5 days prior to the transect. At the time that the image was made, our cruise track would have crossed the northern front at a right angle but the crossing of the southern front would have been made at a more oblique angle. It is quite possible that our perception of a diffuse southern front may be the result of an oblique crossing angle.

Contours of temperature, salinity, and density (Fig. 3a–c) reveal the two-dimensional structure (to 150 m) of the CCF. The temperature fronts at the sides of the CCF were also fronts in salinity and density. The locations of the fronts, defined by 15°C SST, were 41°40′N and 42°40′N. Although the northern front was sharp in the upper 30 m, it became more diffuse with depth. Both fronts extended at least to 150 m, where RSVP coverage stopped. The feature was asymmetric, the near surface frontal boundary being much sharper to the north while the isopycnal slopes below 50 m were considerably greater at the southern boundary. Intrusive activity was mostly confined to the frontal boundaries, which showed numerous thermohaline

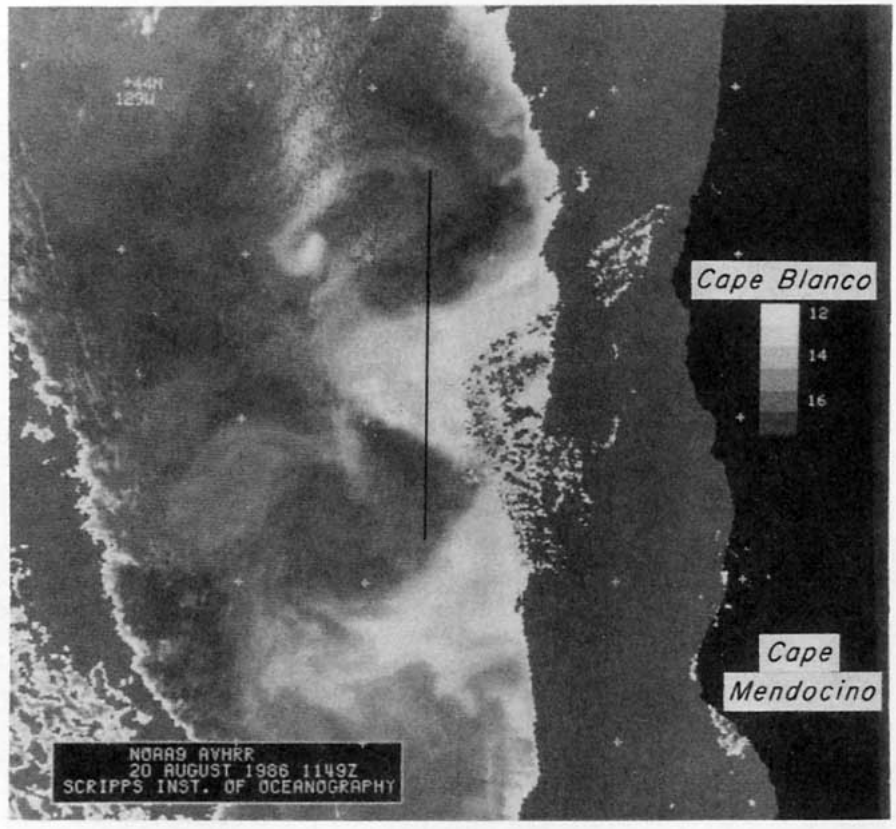

FIG. 1. Infrared signature of the Northern California–Oregon coastline taken by the NOAA 9 satellite on 20 August 1986 at 1149 UTC. The large, cold feature south and west of Cape Blanco (42°50′N, 124°38′W) is thought to be the same feature observed from shipboard on 23 and 24 August 1986. Unfortunately, we could obtain no clear image closer in time to the measurements. The coastline is obscured by clouds to 50–100 km offshore. The track of the transect is indicated by the vertical line. The crosses represent a 1° grid.

intrusions (Fig. 3a, b). The isopycnals (Fig. 3c) showed these intrusions to be stable. In a 30-km wide core centered at 42°05′N the isopycnals had near-zero mean slope and intrusive activity was considerably weaker than in the frontal regions of large isopycnal slopes. Also, vertical excursions of isopycnals were much larger than outside the CCF. This may have been caused either by internal waves or by interleaving of layers over large scales. Since intrusive activity was considerably weaker in this region, and vertical density profiles indicate that the water column was statically stable on scales of the vertical excursions, it appears that the excursions were due to enhanced internal wave activity on horizontal scales of several to tens of kilometers (or to shorter internal waves aliased into those scales by the sampling scheme).

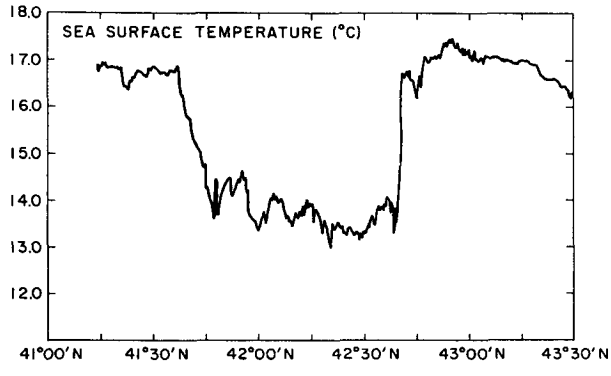

FIG. 2. Sea surface temperature taken from the sea chest (3 m depth) of the R/V *Thompson* during a transect moving southward along 126°30′W beginning 0900 local time 23 August and ending 1300 local time 24 August.

Flow was westward (offshore) over the upper 300 m north of 42°N and eastward (onshore) over the upper 300 m south of 42°N (Figs. 3d and 4). Two high-velocity regions lay in the upper 50 m at the frontal boundaries. Westward currents faster than 70 cm s^{-1} were observed at the northern front associated with high vertical shear (Δu = 30 cm s^{-1} over the depth range 20 to 50 m yields a vertical shear of 0.01 s^{-1}). This shear is likely underestimated because of the filtering of the velocities, but even so it compares in mag-

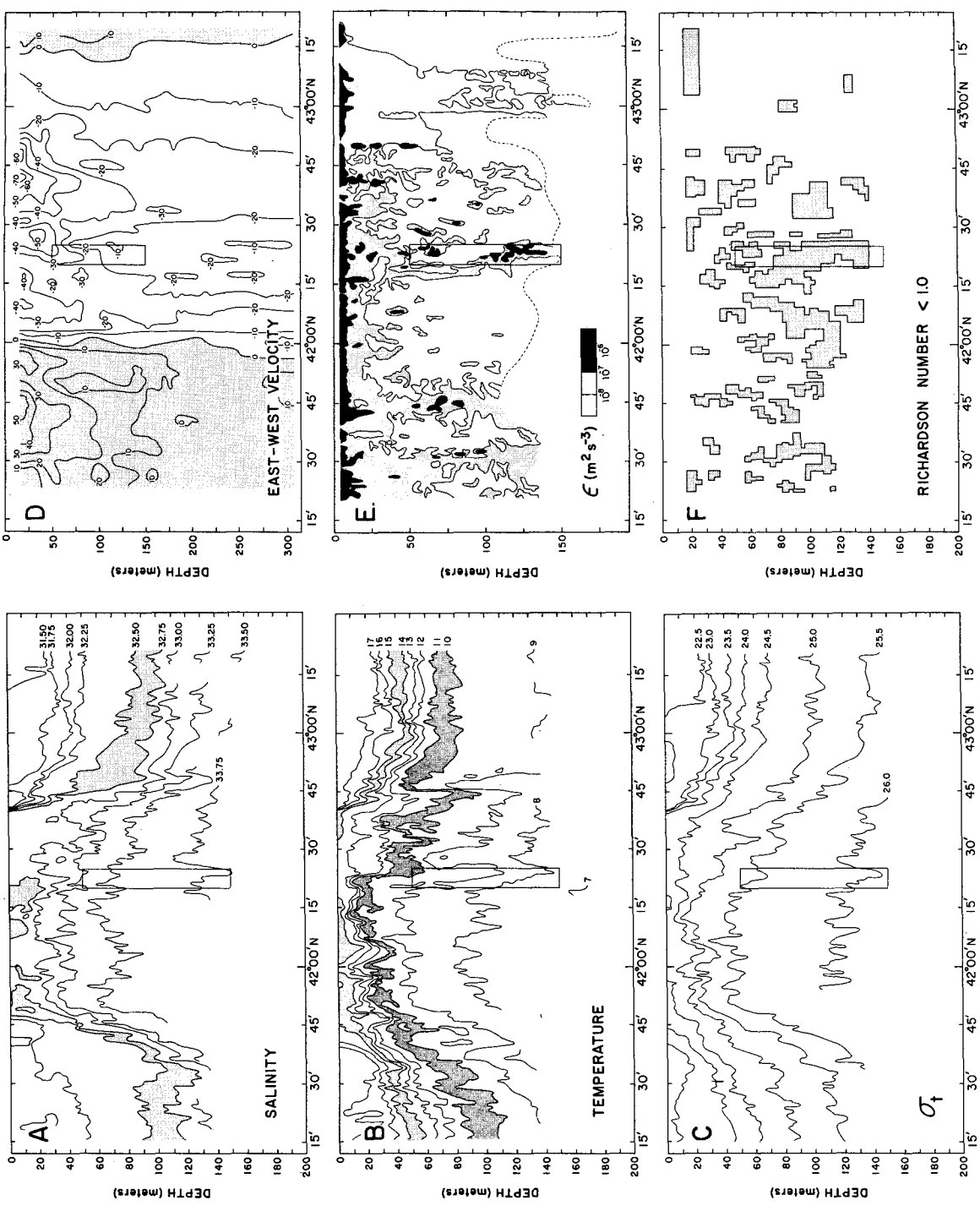

FIG. 3. (a) Isohaline depths calculated using every RSVP profile from the southward transect along 126°30'W. Contour intervals are 0.25 psu. The depth range between 32.50 and 32.75 psu is shaded to emphasize the range of the salinity signature of the feature. (b) Isotherm depths at intervals of 1°C. The water between 10 and 11 degrees is shaded to show more clearly the region of intrusions at the northern side of the feature. (c) Isopycnal depths at intervals of 0.5σ_t. (d) Isotachs of EW velocity from the Doppler profiler. ADCP velocities were referenced using Loran-C navigation, and filtered over 1 hour. Contour interval is 10 cm s^{-1}. Eastward (shoreward) velocities are stippled. (e) Isopleths of kinetic-energy dissipation rate in decades. The dashed line indicates the depth extent of RSVP profiles. (f) Shaded areas in this plot indicate regions where Richardson number is less than 1. Here Richardson number is calculated from the ADCP shear and the RSVP density which has been vertically filtered to match the ADCP data. The depth extent of the data is as indicated in (e). The boxes in each figure correspond to the expanded plot in Fig. 7.

nitude with the vertical shear found in the upper equatorial ocean where the South Equatorial Current flows over the Equatorial Undercurrent (Moum et al. 1986). Westward currents of almost 30 cm s^{-1} were found at 300 m depth below the northern frontal boundary. A second subsurface westward velocity maximum (>50 cm s^{-1}) was observed 15 km south of the front.

Eastward currents as fast as 50 cm s^{-1} were present at the southern boundary. Zonal volume transport estimated from east–west velocities is 7.5×10^6 m^3 s^{-1} westward and 2.6×10^6 m^3 s^{-1} eastward resulting in a net transport of 4.9×10^6 m^3 s^{-1} offshore (Fig. 3d; Table 1; using data to 300 m depth with the velocity in the upper 17 m set equal to the velocity at 17 m; and neglecting the short, separated segment at the far northern end of the transect). The offshore transport is greater because of the larger span of the offshore current (50% larger), and because of the considerably greater westward currents below 100 m.

South of the CCF, flow was southward and eastward (Fig. 4), whereas north of the CCF the water flowed northward and westward. The northern frontal boundary was a region of strong meridional convergence. Northward currents of 50 cm s^{-1} 15 km south of the front abruptly became zero at the frontal boundary. Downwelling at the front due to the meridional convergence is possible, but it is likely that most of the meridional convergence is accounted for by the offshore flow. At the northern frontal boundary, meridionally convergent flow was observed at all depths sampled.

The combined evidence of the satellite infrared image (Fig. 1), the density contours (Fig. 3c), and the velocity field (Figs. 3d and 4) suggests an image of a single, large, cold feature rotating in the cyclonic direction. The feature is either an eddy which has pinched off from the coastal jet at the upwelling/open ocean front or is a meander of the coastal jet. Due to cloud

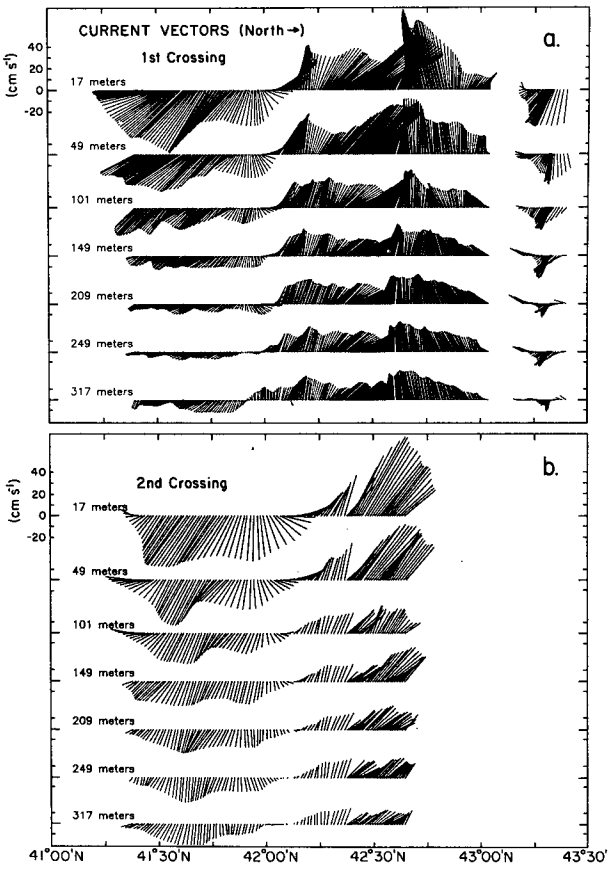

FIG. 4. Current vectors at selected depths to 317 m. Vectors have been rotated so that northward currents are to the right. (a) First transect at 4.5 kt. (b) Second transect at 11 kt. The 5 min averaging of ADCP velocity profiles shows as an increased separation between vectors. At 42°22'N, there is a discontinuity of several hours in measurements after which we proceeded northward at about 4 knots.

TABLE 1. Westward transports measured by acoustic Doppler current profiler on the first transect, categorized at 100 m depth intervals and 0.1 degree latitude intervals, in units of 10^6 m^3 s^{-1}.

Latitude (°N)	0–100 (m)	100–200 (m)	200–300 (m)	0–300 (m)
41.45	−0.17	−0.10	−0.04	−0.31
41.55	−0.31	−0.10	−0.05	−0.46
41.65	−0.37	−0.11	−0.05	−0.53
41.75	−0.39	−0.10	−0.08	−0.57
41.85	−0.23	−0.11	−0.09	−0.43
41.95	−0.23	−0.09	0.00	−0.32
42.05	0.14	0.13	0.13	0.40
42.15	0.39	0.26	0.26	0.91
42.25	0.33	0.22	0.22	0.77
42.35	0.35	0.17	0.20	0.72
42.45	0.40	0.16	0.17	0.73
42.55	0.43	0.29	0.27	0.99
42.65	0.55	0.28	0.32	1.15
42.75	0.48	0.25	0.30	1.03
42.85	0.35	0.21	0.23	0.79
Cumulative	1.72	1.36	1.79	4.88
	35%	28%	37%	

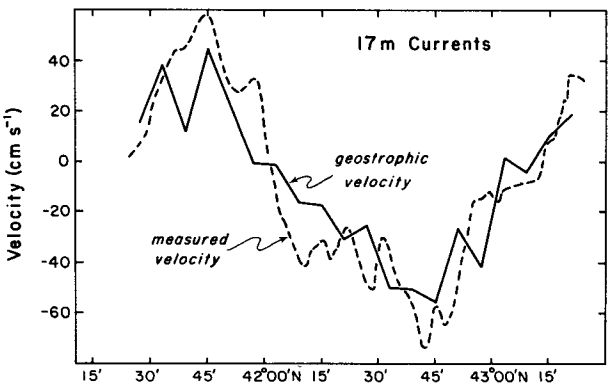

FIG. 5. East–west currents ($E > 0$) at 17 meters depth. The dashed line represents measured (ADCP) currents, solid line represents 0.1° estimates of geostrophic currents relative to 117 m depth, and referenced to the ADCP currents at 117 m.

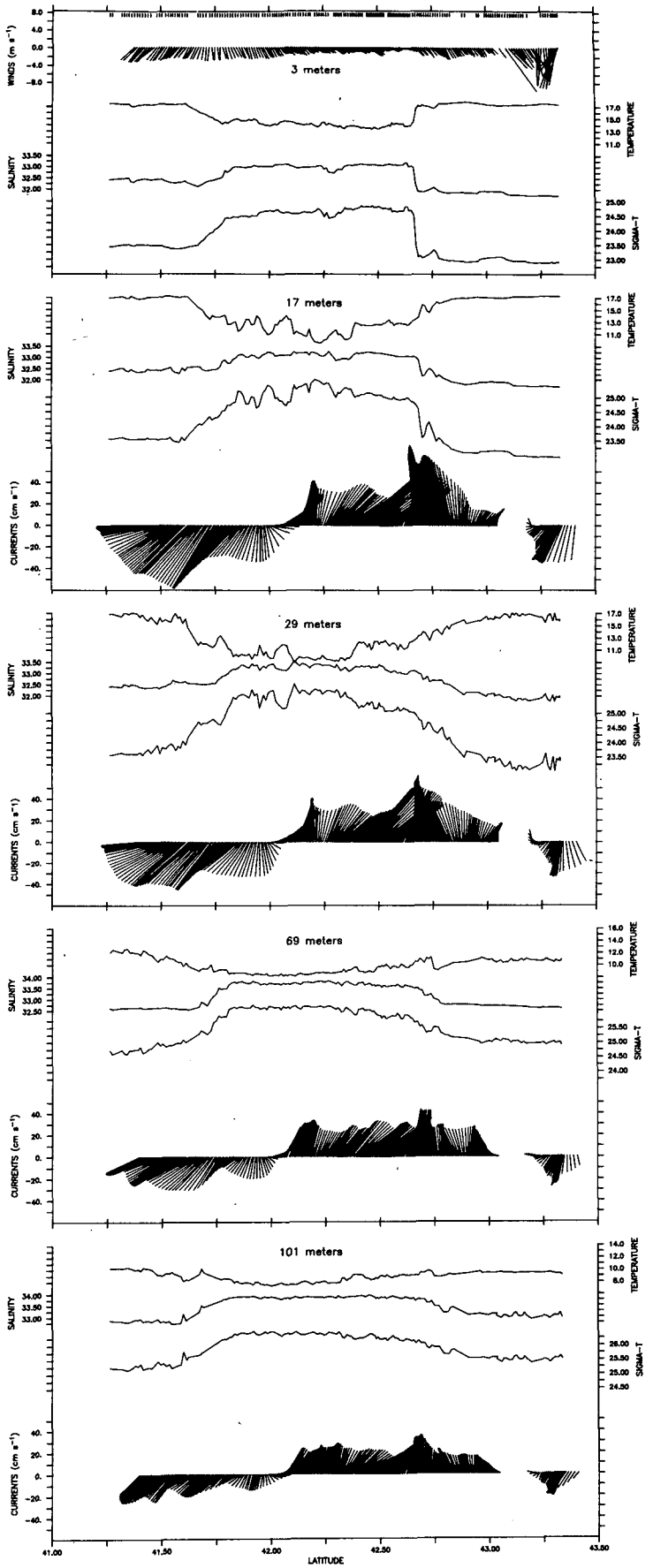
3 meters
17 meters
29 meters
69 meters
101 meters
WINDS (m s⁻¹)
SALINITY
TEMPERATURE
SIGMA-T
CURRENTS (cm s⁻¹)
LATITUDE
41.00
41.50
42.00
42.50
43.00
43.50

cover near the coast in the satellite image (Fig. 1) it is not possible to establish whether the feature is continuous with the coastal upwelling zone (as a meander would be) or not (an eddy). Recent evidence from the Coastal Transition Zone experiment (Kosro and Huyer 1987) suggests that many of the jetlike features found off the coast of northern California are in fact meanders of the coastal jet. We suspect this may be an example of such a meander.

Because of the highly rotational nature of this feature we did not expect a simple geostrophic balance to hold, but the observed geostrophic currents agree well with measured velocities (Fig. 5; 75% of the variance in the measured velocity at 17 m was accounted for by the estimated geostrophic velocity referenced to 117 m). Ring balances include a significant centripetal term (Joyce 1984; Kunze 1986), but in this case any centripetal contribution to the momentum balance is at best a second-order correction. Within measurement error this flow is geostrophic on scales of 10 km and greater.

One gains a somewhat different perspective by examining properties along pressure surfaces (Fig. 6; here temperature and salinity have been scaled to represent equal contributions to density). At the sharp northern front, the surface (3 m) density contrast was almost equally due to temperature and salinity. The contribution due to temperature decreased with depth, so that by 100 m the density was largely determined by salinity. At 100 m the core of the feature was saltier (approximately 34.0 psu) than its surroundings (<33.0 psu). The variability of T, S and σ_t along a pressure surface was larger at 17 and 29 m within the feature than at other depths or outside the feature. Stratification was greatest at these depths. Near the surface we expect a vertically well-mixed layer, hence the horizontal uniformity along the 3 m surface. Below 50 m, the stratification decreased significantly. At intermediate depths, then, we expect to find the greatest amount of internal wave activity and it was possibly the manifestation of enhanced internal wave activity that was observed in the well-stratified depth range (17, 29 m) within the CCF.

4. Signature of the Northern Front

Northern-boundary profiles indicate the dramatic horizontal gradients near the surface and the shallowness of the sharp surface manifestation of the feature (Fig. 7). These four profiles, obtained within 30 minutes, covered 4 km. The largest horizontal gradients were confined to the upper 10 m (Fig. 6 shows the mean gradient to be substantially smaller at 17 m than at 3 m). The 6 m thick near-surface mixed layer of warm freshwater north of the front (profile 28/52) indicates the depth of the SST front. Regrettably, we have no measure of currents in the upper 15 m. We suspect there was a large relative motion along the near-surface horizontal density gradient as the buoyant surface plume presumably flooded over the denser CCF water. If true then large values of turbulent dissipation, ϵ, (28/52—peak values $> 10^{-6}$ m^2 s^{-3}) may have been due to shear instabilities at the bottom interface of the flooding plume. Profiles 28/53 and 28/54 indicate the frontal transition region. Even on the scale of Fig. 7, instabilities in the density structure near the surface are apparent. Unfortunately, possible contamination by the ship's wake precludes a closer look at the near-surface data.

Intrusions are evident in vertical profiles (Fig. 7). A cool fresh intrusion at 95 m in 28/53 and 28/54 overlays an actively-mixing patch ($\epsilon \approx 10^{-7}$ m^2 s^{-3} over several meters). Nearer the CCF (28/54) the warm salty layer above the cool fresh intrusion may have been associated with the intrusion at 80 m in 29/01. The most distinctive feature is the 3 m thick cool ($\Delta T = 0.5$°C), fresh ($\Delta S = 0.2$ psu) intrusion at 50 m in 29/01. In a rapidly evolving flow such as this, the mixing associated with this and other intrusions noted in Fig. 7 is likely shear-driven and only weakly dependent on double-diffusive processes. In the next section we examine a large intrusion in more detail.

5. Mixing and intrusions

During the 28-hour period of the transect, no increase in upper ocean ϵ after sunset occurred; there was no effect resembling the well-developed diurnal cycle of upper-ocean mixing at the equator (Moum and Caldwell 1985; Gregg et al. 1985). Winds were light (Fig. 6; 2–4 m s^{-1}) during the transect. Before 23 August, winds were more normal for the time of year (8–12 m s^{-1}) and at that time we did see a definite increase in ϵ following the change in surface buoyancy flux at sundown. The wind plays an important role in modulating the diurnal mixing (Moum and Caldwell 1985); this may have been an occasion when the wind was too light to support the cycle.

In the top 20 m, ϵ exceeded 10^{-8} m^2 s^{-3} throughout the CCF. In deeper waters, stronger dissipation appears near the frontal boundaries at 41°40′ and 42°40′N and in the subsurface velocity maximum at 42°20′N. The vertical shear in the upper 75 m was large in these regions (Fig. 4); the mixing may have been related to

FIG. 6. Temperature, salinity, and σ_t at 3, 17, 29, 69 and 101 m depth. Wind speed vectors are shown at the top; current vectors are shown at 17 m and below (wind and current vectors are northward to the right). Temperature and salinity have been scaled to represent equal contributions to density. Ticks across the top represent locations of RSVP profiles.

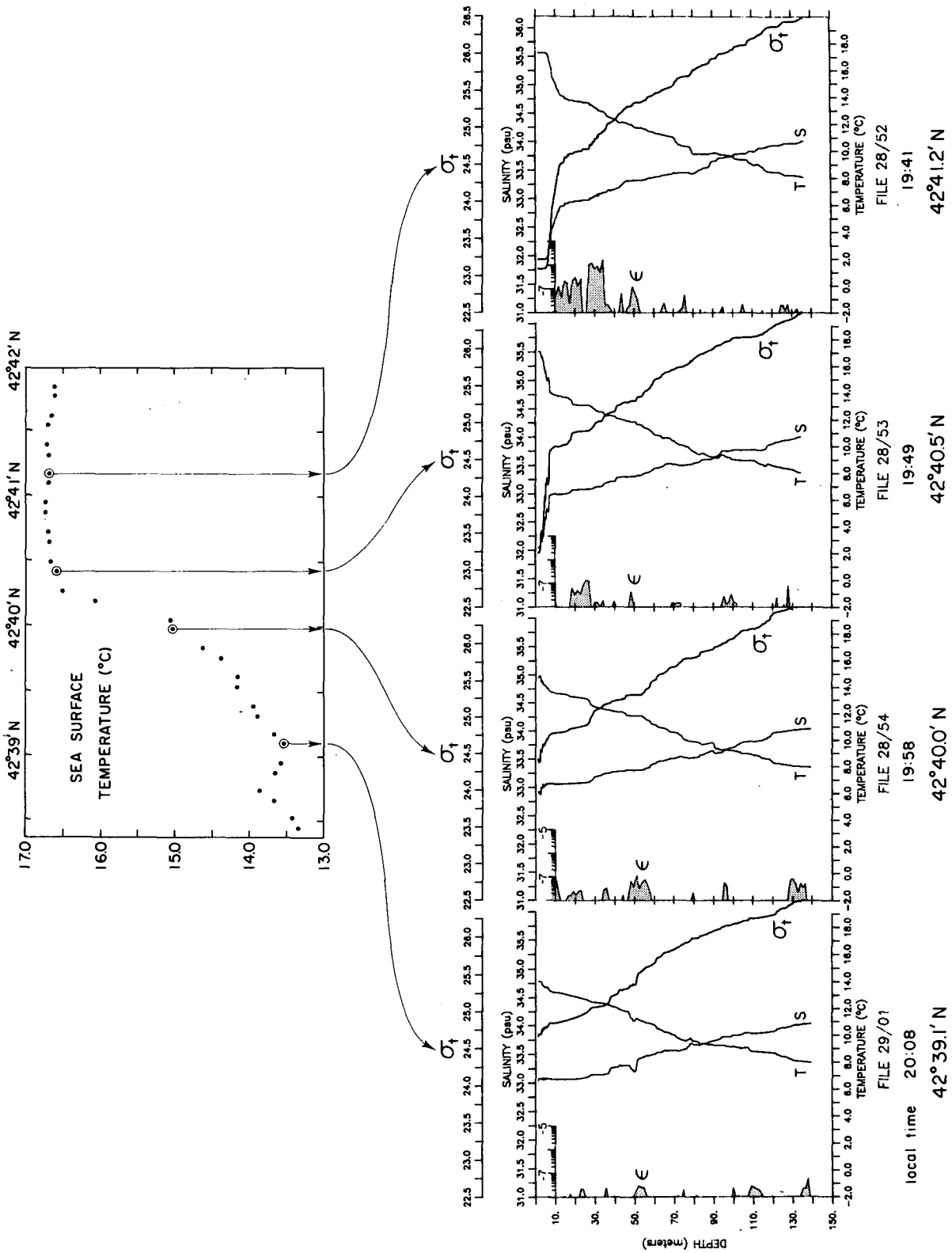

FIG. 7. Four profiles of T, S, σ_t and ϵ through the northern frontal boundary, associated with their positions on the SST plot. Times and latitudes of profiles are noted below each. The logarithm of ϵ is plotted in units of $m^2 s^{-3}$.

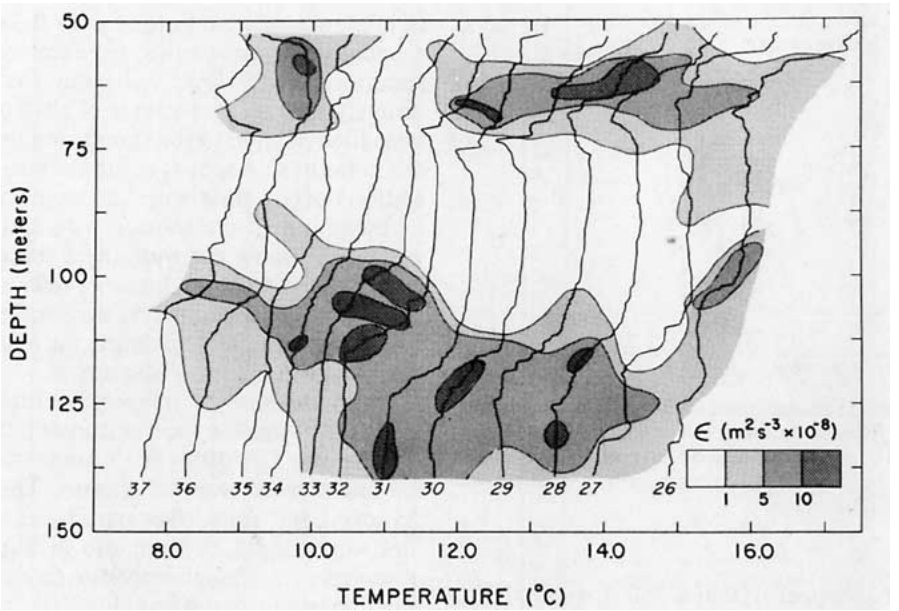

FIG. 8. Temperature profiles in the region indicated by the boxes in Fig. 3. The profiles are spaced approximately at 1 km intervals. They have been offset for clarity. The temperature scale is relative. Contours of ϵ have been fitted to the temperature profiles. Profiles 28–33 show clearly the well-defined intrusion of relatively warm, salty water between 75 and 110 m.

this shear (either directly via shear instabilities or perhaps indirectly via internal wave enhancement within the high shear zone). Within the core, the region of near-zero mean isopycnal slope (30 km centered at 42°05′N; section 3) which encompassed the center of east–west rotation in this transect, there was a relatively "dead" zone. Below 30 m, ϵ rarely exceeded 10^{-8} $m^2 s^{-3}$.

We have noted the relative lack of intrusive activity within the "dead" zone in the core (Fig. 3) and the enhanced intrusive activity nearer the frontal boundaries and have associated a number of intrusions directly with active mixing (Fig. 7). The vertical structure of the water column shown in RSVP profiles revealed numerous instances of intrusive activity linked to mixing. A particularly notable example was the patch cen-

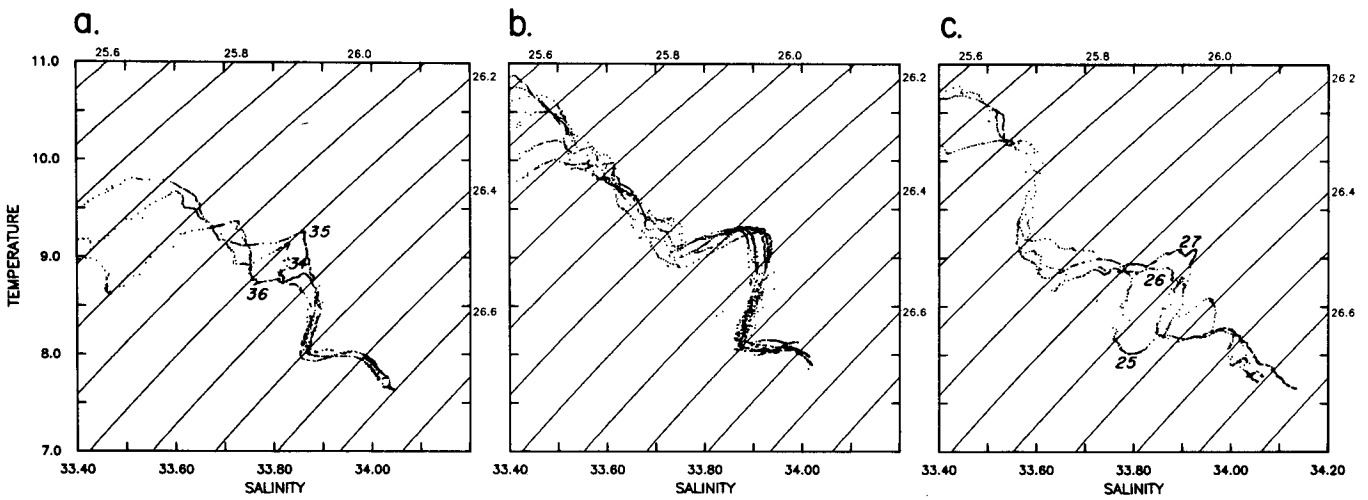

FIG. 9. *T–S* plots corresponding to the casts shown in Fig. 7. (a) Profiles 34–36; (b) 28–33; (c) 25–27. Units of σ_t on the top and right-hand axes correspond to lines of constant density drawn from lower left to upper right. The six profiles in (b) are not labeled since they are so nearly indistinguishable from each other. Note the progression of *T–S* profiles away from the well-defined properties between 26.2 and 26.4σ_t units with distance from the intrusion.

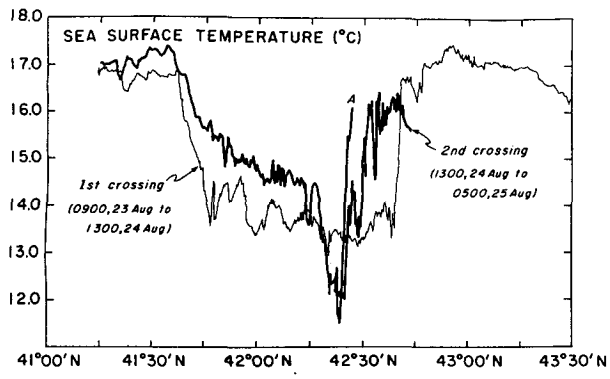

FIG. 10. SST from the second (northward) transect (heavy line), which immediately followed the first southward transect (light line). The feature denoted by *A* corresponds to the first northward encounter with the front. Having crossed it, we reversed course, recrossed it and proceeded slowly northward again.

tered at 42°22'N between 110 and 140 m depth. (The rectangular boxes in Fig. 3 correspond to a region which encompasses this patch. An expanded representation of temperature profiles and ϵ contours is shown in Fig. 8.) This actively mixing patch with no obvious link to the surface ($\epsilon > 3 \times 10^{-7}$ m^2 s^{-3}) was 30 m thick and about 7 km wide (aspect ratio $\approx$ 200). Such a patch might be caused by persistent mixing due to near-inertial internal waves (Gregg et al. 1986), but the only test we could make with our data (depth rotation of relative current vectors) did not bear this out. Rather, this phenomenon appears to be directly linked to a large warm, salty intrusion moving rapidly relative to its surroundings. We do not have absolute velocity measurements on a time scale appropriate to examine the detailed velocity structure of the intrusion. Unaveraged velocity shear, however, indicates relative motion at top and bottom of the feature. The shear estimates also indicate occasional large values within the intrusion itself, so the result is not clear.

Twelve profiles spaced 1–2 km apart through and on either side of the patch reveal the nature of this intrusion (Fig. 8). The six middle profiles in this series show a tightly-knit *T–S* relation between 8.0° and 9.5°C and 33.6 and 34.0 psu (Fig. 9). The intrusion was confined to density surfaces, but not to pressure surfaces. In fact, it experienced considerable vertical straining, perhaps by gravitational oscillations.

6. Second transect

In attempting to characterize the spatial extent of the CCF feature, or patches within the feature, we are limited by the inherent space–time aliasing of single-point sampling. We have presented our data as a spatial cross section but cannot detail the temporal evolution. For example, the patch noted in the previous section was characterized as 7 km in horizontal extent. This, of course, represents our perception of its size in a frame of reference relative to the earth. Relative to the ship, we observed a patch whose time scale was several hours (many times the local buoyancy frequency). Unfortunately, our measurements of absolute velocity have been filtered (due to the smoothing required to reduce the noise in ship speeds computed from Loran-C navigation) over a time scale too large to permit detailed investigation of the motion within the patch. Hence we do not know the motion of the water within the patch relative to either frame of reference. Recognizing our lack of information on time scales, we performed a second experiment to define the changes in SST and currents over a period of a day.

Upon finishing the transect, we immediately turned around and made a second transect, this time heading north along 126°30'N at 11 knots (ship speed during the first transect was 4.5 knots). The RSVP was not deployed, but sea surface parameters and ADCP profiles were logged. A dramatic evolution in SST was observed even though only one day separated the second transect from the first (Fig. 10). The southern SST frontal boundary was considerably more diffuse. The SST was $\approx$1°C warmer within the CCF south of 42°15'N, and the coldest surface water (11.5°C) was observed at 42°25'N. The northern boundary of the surface front had migrated southward 27 km when first observed on the second transect. With the intention of deploying the RSVP and moving slowly through the front in hopes of examining it in detail, we backtracked to a position south of the front and attempted to recross it. By the time we finally found the front some *6 hours* later, it had evolved radically and moved *8 km northward!*

Current vectors from second-transect ADCP profiles (Fig. 4b) did not exhibit as radical a departure from the first transect (Fig. 4a) as did the structure of SST. In fact, the spatial pattern of currents changed little, although the strength of shoreward return flow increased greatly and the meridional convergence at the northern boundary weakened. The net volume transport for the second transect cannot be estimated because the transect was not complete.

7. Discussion and summary

Limitations on available satellite imagery and ship time (to obtain more, detailed transects) make it difficult to determine clearly the large scale form of this cold core feature. Certainly, it was more coherent and regular than any of the features observed off Point Arena. It also exhibited opposing flows (offshore at the northern front, onshore at the southern front). Rather than being jetlike, the feature resembles an eddy or meander. Based upon more recent measurements (Kosro and Huyer 1987) we suspect that this feature is a meander of the coastal jet which is ubiquitous at the front separating cold, upwelled nearshore water from warmer, open ocean water (Huyer 1983). This

makes the model of Ikeda and Emery (1984) appealing as a dynamical representation of our observations.

We suspect that the rapid evolution of SST between the two transects was due to a number of factors. The contribution of horizontal advection must be significant since both east–west and north–south velocities were so large near the fronts. However, the evolution of the near-surface water was apparently greater than one would expect when compared to that indicated by successive velocity transects and may be considerably greater than that of the subsurface waters at the fronts. Certainly, the signature of the front at 3 m is sharper than that below 3 m. Profiles across the northern frontal boundary indicate the transition of the near-surface pycnocline which is due to the relative weakening with depth of the frontal gradients. Perhaps the near-surface waters above the pycnocline can be characterized as a buoyant surface plume since they are so much lighter than both the water below and that within the CCF.

In summary, a large and coherent feature off Cape Blanco exhibited

1) changes in SST as large as 2 degrees in 1 km (and smaller gradients at depth);
2) an eddy- or meander-like structure in mean currents;
3) a geostrophically-balanced current field over scales of 10 km and greater;
4) intrusive activity at frontal boundaries;
5) a concentration of turbulent mixing at the edges of the feature and associated with intrusions, the core of the feature being turbulence-free; and
6) significant changes in surface structure between observations separated by 24 hours.

Acknowledgments. This research was supported by the National Science Foundation under Grant OCE-8214639 and the Office of Naval Research under Contract N00014-87-K-0242. The efforts of Terry Sullivan in processing the navigation, SST and wind data are gratefully acknowledged. Ted Strub helped us to obtain a clear satellite image. We are also indebted to Melora Park, Meroe Park, Mike Brown, Rich Schramm, Marc Willis, Jutta Richter, Erik Fields, Fred Bahr, and Terry Sullivan, as well as Captain Clampitt and the crew of the R/V *Thomas G. Thompson* for their help at sea. George White made a tremendous contribution in ensuring that we had a working ADCP transducer for our cruise. Jane Huyer, Ted Strub, and Ken Brink made valuable comments on an earlier version of this manuscript.

REFERENCES

Bernstein, R. L., L. Breaker and R. Whritner, 1977: California current eddy formation: Ship, air and satellite results. *Science,* **195,** 353–359.

Caldwell, D. R., T. M. Dillon and J. N. Moum, 1985: The Rapid Sampling Vertical Profiler: an evaluation. *J. Atmos. Oceanic Technol.,* **2,** 615–625.

Flament, P., L. Armi and L. Washburn, 1985: The evolving structure of an upwelling filament. *J. Geophys. Res.,* **90,** 11,765–11,778.

Gregg, M. C., E. A. D'Asaro, T. J. Shay and N. Larson, 1986: Observations of persistent mixing and near-inertial internal waves. *J. Phys. Oceanogr.,* **16,** 856–885.

Huyer, A., 1983: Coastal upwelling in the California Current system. *Progress in Oceanography,* Vol. 12, Pergamon 259–283.

Ikeda, M., and W. J. Emery, 1984: Satellite observations and modelling of meanders in the California current system off Oregon and northern California. *J. Phys. Oceanogr.,* **14,** 1434–1450.

Joyce, T. M., 1985: Velocity and hydrographic structure of a Gulf Stream Warm Core Ring. *J. Phys. Oceanogr.,* **14,** 936–947.

Kelly, K. A., 1985: The influence of winds and topography on the sea surface temperature over the northern California slope. *J. Geophys. Res.,* **90,** 11 783–11 798.

Kosro, P. M., and A. Huyer, 1986: CTD and velocity surveys of seaward jets off northern California. *J. Geophys. Res.,* **91,** 7680–7690.

——, and ——, 1987: Preliminary results of ADCP/CTD surveys in May and June 1987. *Coastal Transition Zone Newslett.,* **2(4),** 4–12.

Kunze, E., 1986: The mean and near-inertial velocity fields in a Warm-Core Ring. *J. Phys. Oceanogr.,* **16,** 1444–1461.

Mooers, C. M. K., and A. R. Robinson, 1984: Turbulent jets and eddies in the California current and inferred cross-shore transports. *Science,* **223,** 51–53.

Moum, J. N., and D. R. Caldwell, 1985: Local influences on shear turbulence in the equatorial ocean. *Science,* **230,** 315–316.

——, T. R. Osborn and W. R. Crawford, 1986: Pacific equatorial turbulence: revisited. *J. Phys. Oceanogr.,* **16,** 1516–1522.

Osborn, T. R., and W. R. Crawford, 1980: An airfoil probe for measuring turbulent velocity fluctuations in water. *Air–Sea Interaction—Instruments and Methods.,* F. Dobson, L. Hasse and R. Davis Eds, Plenum Press.

Reinecker, M. M., and C. N. K. Mooers, 1985: A cool anomaly off northern California: An investigation using IR imagery and in situ data. *J. Geophys. Res.,* **90,** 4807–4818.